Original Article

# Correlation between Condylar Fracture Pattern after Parasymphyseal Impact and Condyle Morphological Features: A Retrospective Analysis of 107 Chinese Patients

**Lu Han[1,2], Ting Long[2], Wei Tang[2], Lei Liu[2], Wei Jing[2], Wei-Dong Tian[2], Jie Long[1,2]**

[1]State Key Laboratory of Oral Diseases, Sichuan University, Chengdu, Sichuan 610041, China
[2]Department of Oral and Maxillofacial Surgery, West China School of Stomatology, Sichuan University, Chengdu, Sichuan 610041, China

## Abstract

**Background:** The treatment of the condylar fractures is difficult. Factors that result in the fractures are complex. The objective of this morphometric study was to investigate the relationship between condylar fracture patterns and condylar morphological characteristics.
**Methods:** We conducted a retrospective analysis of 107 patients admitted to the West China Hospital of Stomatology for bilateral condylar fractures caused by parasymphyseal impact. The patients were divided into five groups according to the type of condylar fracture. Ten parameters were evaluated on three-dimensional (3D) reconstruction mandible models through the Mimics 16.0 (Materialize Leuven, Belgium) anthropometry toolkit. Each parameter of the 3D models was analyzed using multivariate analysis. Multinomial logistic regression analyses were used to examine the relationships between the five groups.
**Results:** The results showed that the differences of condylar head width (M1), condylar neck width (M3), the ratio of condylar head width to condylar anteroposterior diameter (M1/M2), the ratio of condylar head width to condylar neck width (M1/M3), the ratio of condylar height to ramus height (M8/M7), and mandibular angle (M10) were statistically significant ($p < 0.05$). Type A condylar head fractures were positively associated with M1 (compared to Type B: OR =1.627, 95% CI: 1.123, 2.359; compared to Type C: OR = 1.705, 95% CI: 1.170, 2.484) and M1/M2 (compared to Type B: OR =1.034, 95% CI: 0.879, 2.484). Type B condylar head fractures were negatively associated with M10 (compared to Type C: OR = 0.909, 95% CI: 0.821, 1.007). Condylar neck fractures were negatively associated with M3 (compared to condylar head: OR = 0.382, CI: 0.203, 0.720 ; compared to condylar base: OR = 0.436, 95% CI: 0.218, 0.874), and positively associated with M1/M3 (compared to condylar head: OR = 1.229, 95% CI: 1.063, 1.420 compared to condylar base: OR = 1.223, 95% CI: 1.034, 1.447). Condylar base fractures were positively associated with M10 (OR = 1.095, 95% CI: 1.008, 1.189) and negatively associated with M8/M7 (OR = 0.855, 95% CI: 0.763, 0.959) as compared with condylar head fractures.
**Conclusions:** Condylar fracture pattern is associated with the anatomical features of the condyles when a fracture occurs from parasymphyseal impact.

**Key words:** Anatomical Feature; Condylar Fracture; Parasymphyseal Impact; Three-dimensional Reconstruction

## Introduction

Mandible fractures are the most common fractures when facial trauma occurs and they account for approximately 23.8–81.3% of all maxillofacial fractures.[1-3] The main causes of facial fractures are car accidents, assaults, and sports-related injuries. Condylar fractures account for 17.5–52.0% of all mandibular fractures.[4] Studies of condylar fractures consistently update etiological information.[3-7] Zhou *et al*.[5] reported that the location of mandibular fractures is strongly correlated with age, sex, soft-tissue injuries, and dental trauma. However, most of the studies lack information about anatomical factors.

Access this article online

Quick Response Code:

Website: www.cmj.org

DOI: 10.4103/0366-6999.199836

**Address for correspondence:** Prof. Jie Long, Department of Oral and Maxillofacial Surgery, West China School of Stomatology, Sichuan University, Chengdu, Sichuan 610041, China
E-Mail: dr.jielong@hotmail.com



**Received:** 19-10-2016 **Edited by:** Yi Cui
**How to cite this article:** Han L, Long T, Tang W, Liu L, Jing W, Tian WD, Long J. Correlation between Condylar Fracture Pattern after Parasymphyseal Impact and Condyle Morphological Features: A Retrospective Analysis of 107 Chinese Patients. Chin Med J 2017;130:420-7.

The development of digital surgery techniques has provided a number of valid methods for morphological study. Researchers have come to understand the importance of internal factors that influence fracture patterns such as mandibular anatomy, bone mineral density, and masticatory muscles. Considering that morphological variation is a factor that could influence fracture type, the purpose of this study was to evaluate the relationship between condylar morphology and condylar fracture patterns that occur because of parasymphyseal impact. We believe that a comprehensive understanding of the various factors that influence the location of mandibular fractures may provide new guidelines for the prevention and treatment of such fractures.

Several recent finite element analysis (FEA) studies have examined the biomechanical behavior of the mandible when trauma occurs.[8-11] The studies have described the distribution of compressive forces and tensile stresses and reported the presence of potentially weak areas in the mandibular geometry. Huelke and Harger[12] found that fractures occur more readily under tension than compression. In the case of a frontal blow, a jaw with fracture at the impact point acts like a lever.[13] The compressive stress is mainly distributed in the mandibular angle and posterior aspect of the condyle bilaterally through the mandibular body and ramus axis, in addition to the impact point. Xin *et al*.[14] reported that condylar head fractures after parasymphyseal impact are related to the anatomical features of the condyles.

Because of the limitations in obtaining measuring directly on a real mandible *in vivo*, investigations have concentrated on three-dimensional (3D) reconstruction mandible models. Spiral computerized tomography, as a comprehensive radiographic tool, has the ability to render 3D head models, allowing linear, angular, and volumetric measurements of the facial skeleton. The accuracy of these techniques has been verified in previous studies.[15,16] In addition, computer-aided surgical simulation (CASS) based on computed tomography (CT) is an established technique widely used for treatment planning and surgical navigation. Tucker *et al*.[16] verified the reliability and accuracy of 3D surgical simulations by comparing the simulated outcomes with the actual models. They quantified the differences and reported that none were statistically significant. Thus, a 3D model, as a true representation of reality, allows researchers and clinicians to obtain more precise results when compared to conventional techniques.

The objective of this morphometric study was to investigate the relationship between condylar fracture patterns due to parasymphyseal impact and condylar morphological characteristics. CASS was used to reconstruct condylar morphology in patients with condylar fractures, and ten metrics on the reconstructed models were analyzed for correlations with fracture patterns.

## Methods

### Clinical data

This study was carried out at the West China Hospital of Stomatology, Sichuan University, Chengdu, Sichuan, China. We analyzed the data of 107 patients with bilateral condylar fractures because of a parasymphyseal impact, ranging in age from 20 to 47 years, and seen from June 2013 to July 2016. These patients were identified by a review of the medical records. Inclusion criteria for the analysis were a bilateral condylar fracture due to a parasymphyseal impact and no malignancy or congenital malformation. Included patients were also required to have complete permanent dentition or a maximum of two missing teeth in different quadrants, excluding the third molars.

The fracture classification system of the condylar process used was the system of Lindahl[17] and Neff *et al*.,[18] as shown in Figure 1. Patients were divided into five groups according to the condylar fracture type. Group I: the fracture line starts in the articular surface and may extend through medial part of the condylar head (Type A diacapsular condylar fracture). Group II: fracture line through lateral part of the condylar head (Type B diacapsular condylar fracture). Group III: fracture line near to the attachment of the lateral capsule (Type C diacapsular condylar fracture). Group IV: fracture of the condylar neck, with the fracture line more than half above a perpendicular line through the sigmoid notch to the tangent of the ramus. Group V: fracture of the condylar base, with the fracture line more than half below a perpendicular line through the sigmoid notch to the tangent of the ramus. Patient data were summarized in Table 1.

### Three-dimensional model reconstruction and anthropometric measurements

The spiral CT images (Philips Brilliance 16 CT Scanner, The Netherlands) of the patients were analyzed. All the CT images were stored in DICOM file format on Windows 10-based graphics workstation (Intel Core i5 4600, 8 GB, NVIDIA GeForce GTX 950M), and subsequently imported into Mimics 16.0.

Mimics 16.0 was used to generate computerized composite skull models of the patients, including the skeleton and dentition. We focused on 3D reconstruction of the mandible from CT scan data to produce a final postsurgical working model. A segmentation technique was then applied to each CT mask in the data set to identify and separate the fractured fragments from the surrounding tissues. As the accuracy of virtual surgeries is well known, CASS was performed on every patient. The operator performed the simulation surgery by moving and rotating the digitally customized bony segments according to the fracture line, until the desired surgical outcome was achieved. The intervention was aimed at realignment of the fractured segments into their normal anatomic positions, just as in a clinical surgical procedure. The bony segments were merged with each other at the final desired locations.

We selected 13 landmarks on each side of the 3D mandible models (L1–L13), which are listed in Table 2 and shown in Figure 2. Landmarks were located and marked by the same trained researchers. Ten parameters [Table 3 and Figure 3], which have been used in a prior study, were measured using the anthropometry toolkit of Mimics16.0. The high

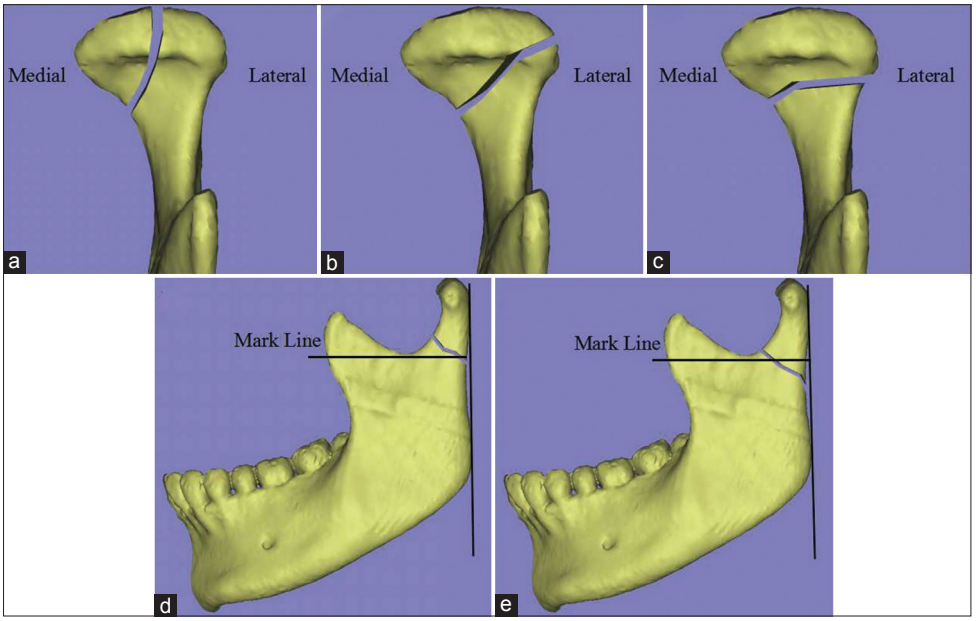


**Figure 1:** Classifications of condylar fractures. (a) Type A diacapsular condylar fracture: the fracture line starts in the articular surface and may extend through medial part of the condylar head. (b) Type B diacapsular condylar fracture: fracture line through lateral part of the condylar head. (c) Type C diacapsular condylar fracture: Fracture line near to the attachment of the lateral capsule. (d) Fracture of the condylar neck. (e) Fracture of the condylar base. Mark line: A perpendicular line through the sigmoid notch to the tangent of the ramus.

**Table 1: Classification and details of each group**

| Groups | Fracture type | *n* | Gender (male/female) | Mean age (years) | Cause of the injury | | |
|---|---|---|---|---|---|---|---|
| | | | | | Traffic accident | Fall | Impact |
| Group I | Type A condylar head fracture | 20 | 12/8 | 25.7 | 10 | 4 | 6 |
| Group II | Type B condylar head fracture | 26 | 20/6 | 30.6 | 10 | 13 | 3 |
| Group III | Type C condylar head fracture | 28 | 19/9 | 27.6 | 12 | 10 | 6 |
| Group IV | Condylar neck fracture | 17 | 12/5 | 40.5 | 4 | 9 | 4 |
| Group V | Condylar base fracture | 16 | 13/3 | 34.2 | 6 | 8 | 2 |

reliability and reproducibility of 3D landmarks have been verified by a number of studies.[19-21] Only measurements on the right side of the mandibles were calculated because the analysis showed no statistically significant differences in the measurements between the left and right sides of the mandibles. All measurements were made twice by one researcher within a 2-week interval. The average score was used for the analysis. The digital micrometer used for making the measurements has a sensitivity of 0.001 mm.

## Statistical analysis

Multivariate analysis of variance (MANOVA) was used to evaluate the statistical significance of each parameter among all groups together, and $P < 0.05$ was considered statistically significant. After that, the least significant difference (LSD) test was used to perform all pairwise comparisons between group means.

Multinomial logistic regression analysis was used to calculate odds ratios (*OR*s) and 95% confidence interval (*CI*s) for the associations between selected parameters and fracture patterns. Four multinomial logistic regression models were used for detailed analysis and comparison. In the first two models, we analyzed the correlation between selected parameters and the three types of diacapsular condylar fractures (Types A, B, and C). In the other two models, we evaluated the associations between each parameter and the three types of condylar fractures (condylar head fracture, condylar neck fracture, and condylar base fracture). Groups I–III were combined as the condylar head fracture group. Model fit was assessed using the Hosmer–Lemeshow (HL) goodness-of-fit test. All the data were analyzed using SPSS software version 20.0 for Windows (IBM, Chicago, IL, USA). A value of $P < 0.05$ was considered statistically significant.

# Results

As shown in Table 4, the mean absolute value of condylar head width (M1), condylar neck width (M3), the ratio of condylar head width to condylar anteroposterior diameter (M1/M2), the ratio of condylar head width to condylar neck width (M1/M3), the ratio of condylar height to ramus height (M8/M7), and mandibular angle (M10) in the five groups was significantly different (all $P < 0.05$).

**Table 2: Definitions of landmarks and planes on the mandible**

| Landmarks and planes | Location | Definitions |
|---|---|---|
| Landmarks | | |
| L1 | Highest point of mandibular condyle | The most protruding point of the top margin of mandibular condyle |
| L2 | Posterior point of mandibular condyle | The most protruding point of the posterior margin of mandibular condyle |
| L3 | Convex point of anterior edge of condylar head | The most protruding point of the anterior margin of condyle |
| L4 | Lateral pole of condyle | The most protruding point of the lateral margin of condyle |
| L5 | Medial pole of condyle | The most protruding point of the medial margin of condyle |
| L6 | Concave point of lateral condylar neck flexure | The most concave point of lateral edge of condylar neck flexure |
| L7 | Concave point of medial condylar neck flexure | The most concave point of medial edge of condylar neck flexure |
| L8 | Concave point of mandibular ramus flexure | The most concave point of the posterior edge of mandibular ramus |
| L9 | Lowest point of the sigmoid notch | The most inferior point of the top margin of sigmoid notch |
| L10 | Convex point of anterior edge of mandibular coronoid process | The most protruding point of the anterior margin of mandibular coronoid process |
| L11 | Posterior protruding point of mandibular ramus | The most protruding point of the posterior margin of mandibular ramus |
| L12 | Concave point of anterior edge of mandibular ramus | The most concave point of the anterior margin of mandibular ramus |
| L13 | Gonion point | The most inferior, posterior, and lateral points on the external angle of the mandible |
| Planes | | |
| Pa | The posterior plane of mandibular ramus | The plane of the posterior margin of ramus |
| Pb | The bottom plane of mandibular body | The plane of the inferior margin of mandible |
| Pc | The horizontal reference plane of condyle | The plane parallel to Frankfort horizontal plane and tangent to the lowest point of sigmoid notch (L9) |
| Pd | The horizontal reference plane of ramus | The plane parallel to Frankfort horizontal plane through gonion (L13) |

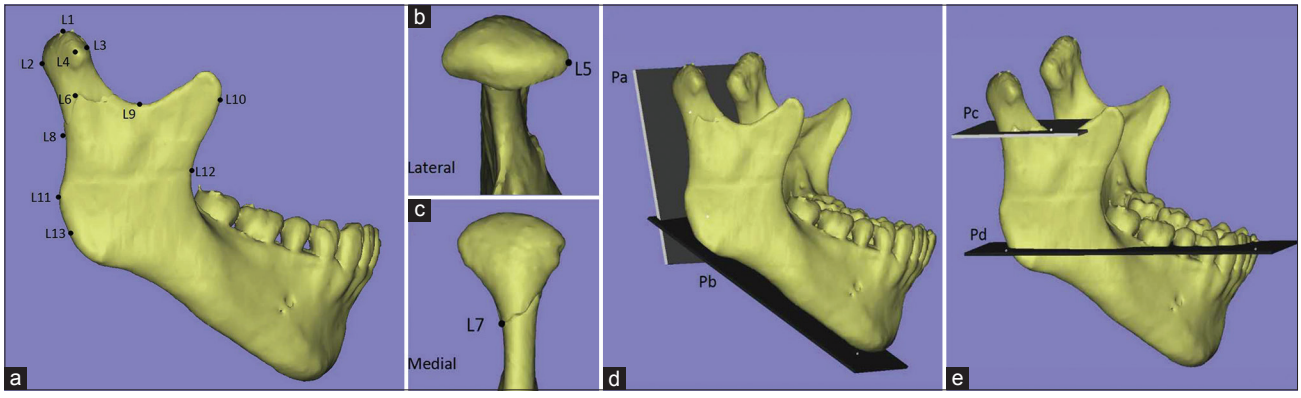


**Figure 2:** Definitions of landmarks and planes of mandibular ramus flexure. (a) L1: Highest point of mandibular condyle. L2: Posterior point of mandibular condyle. L3: Convex point of anterior edge of condylar head. L4: Lateral pole of condyle. L6: Concave point of lateral condylar neck flexure. L8: Concave point of mandibular ramus flexure. L9: Lowest point of the sigmoid notch. L10: Convex point of anterior edge of mandibular coronoid process. L11: Posterior protruding point of mandibular ramus. L12: Concave point of anterior edge of mandibular ramus. L13: Gonion point (lateral view, right side). (b) L5: Medial pole of condyle (top view, right side). (c) L7: Concave point of medial condylar neck flexure (back view, right side). (d) Pa: Posterior plane of mandibular ramus. Pb: Bottom plane of mandibular body (right oblique view). (e) Pc: The horizontal reference plane of condyle. Pd: The horizontal reference plane of ramus (right oblique view).

For M1, statistically significant differences were found between Group I and the other four groups ($P < 0.05$). The mean M1 values of Groups II, III, IV, and V were all less than that of Group I ($P < 0.05$), and the mean M3 value of Group IV was less than that of Groups I, II, and III (all $P < 0.05$). The mean M1/M2 ratio of Group I was significantly greater than that of Group III and Group V (both $P < 0.05$). In addition, the mean M1/M3 ratio of Group IV was greater than that of Groups II, III, and V (all $P < 0.05$). The mean M8/M7 ratio of Group II was significantly greater than that of Group IV and Group V, and the mean M8/M7 of Group I was significantly greater than that of Group V (all $P < 0.05$). M10 of Group I and Group II was significantly less than that of Group III and Group V, respectively (both $P < 0.05$). No differences were detected between M2, M4/M5, M6, and M9 and fracture patterns.

The above-mentioned six parameters were input into the multivariable logistic regression models. In the two models shown in Tables 5 and 6, the HL goodness-of-fit test statistics were 0.46, 0.37, 0.40, and 0.33, respectively, which indicated that the multivariable logistic regression models fit the data well.

According to the first two models, Type A condylar head fractures (compared to Type B fractures) were positively

**Table 3: Definition of measurements on the mandibular ramus**

| Type | Measurements | Abbreviation | Definition |
|---|---|---|---|
| Distance (mm) | M1. Condylar head width | CHW | The maximum distance between the medial (L5) and lateral pole (L4) of condyle |
| | M2. Condylar anteroposterior diameter | CAD | The maximum distance between convex point of anterior edge of condylar head (L3) and posterior point of mandibular condyle (L2) |
| | M3. Condylar neck width | CNW | The minimum distance between concave point of lateral edge of condylar neck flexure (L6) and concave point of medial edge of condylar neck flexure (L7) |
| | M4. Minimum ramus breadth | MIRB | The minimum distance between concave point of anterior edge of mandibular ramus (L12) and concave point of mandibular ramus flexure (L8) |
| | M5. Maximum ramus breadth | MARB | The maximum distance between convex point of anterior edge of mandibular coronoid process (L10) and posterior point of mandibular condyle (L2) |
| | M6. Mandibular flexure depth | MFD | Vertical distance from concave point of mandibular ramus flexure (L8) to posterior plane of mandibular ramus (Pa) |
| | M7. Ramus height | RH | Distance from the highest point of mandibular condyle (L1) to horizontal reference plane of ramus (Pd) |
| | M8. Condylar height | CH | Distance from the highest point of mandibular condyle (L1) to horizontal reference plane of condyle (Pc) |
| Angle (°) | M9. Condylar angle | CA | Angle formed by mandibular flexure's upper border and mandibular flexure's lower border |
| | M10. Mandibular angle | MA | Angle formed by the posterior plane of mandibular ramus (Pa) and the bottom plane of the mandibular corpus (Pb) |

**Table 4: Result of MANOVA for each parameter**

| Parameters | Group I | Group II | Group III | Group IV | Group V | *P* |
|---|---|---|---|---|---|---|
| M1 | 21.040 ± 0.395* | 19.239 ± 0.550 | 19.256 ± 0.532 | 19.623 ± 0.488 | 19.03 ± 0.402 | 0.005 |
| M2 | 9.443 ± 0.249 | 9.081 ± 0.346 | 9.887 ± 0.335 | 9.679 ± 0.308 | 9.634 ± 0.253 | 0.047 |
| M3 | 8.060 ± 0.197 | 7.868 ± 0.274 | 8.039 ± 0.266 | 7.103 ± 0.242† | 7.687 ± 0.201 | 0.030 |
| M1/M2 | 2.244 ± 0.067‡ | 2.196 ± 0.094 | 1.989 ± 0.091 | 2.078 ± 0.083 | 2.000 ± 0.069 | 0.049 |
| M1/M3 | 2.641 ± 0.07 | 2.478 ± 0.098 | 2.428 ± 0.094 | 2.782 ± 0.087§ | 2.504 ± 0.072 | 0.019 |
| M4/M5 | 0.789 ± 0.001 | 0.796 ± 0.009 | 0.771 ± 0.012 | 0.792 ± 0.013 | 0.770 ± 0.092 | 0.238 |
| M6 | 2.432 ± 0.189 | 2.064 ± 0.165 | 2.253 ± 0.205 | 1.870 ± 0.218 | 2.452 ± 0.157 | 0.150 |
| M8/M7 | 0.349 ± 0.01‖ | 0.361 ± 0.008¶ | 0.343 ± 0.011 | 0.328 ± 0.012 | 0.320 ± 0.009 | 0.017 |
| M9 | 163.636 ± 1.709 | 164.710 ± 1.499 | 162.964 ± 1.854 | 166.660 ± 1.974 | 162.718 ± 1.42 | 0.526 |
| M10 | 117.645 ± 1.494‡ | 119.452 ± 1.31‡ | 123.739 ± 1.62 | 121.369 ± 1.725 | 124.629 ± 1.24 | 0.003 |

Data were shown as mean ± SD. *Significant differences were found between this group and the other four groups; †Significant differences were found between this group and Group I, Group II, and Group III; ‡Significant differences were found between this group and Group III and Group V; §Significant differences were found between this group and Group II, Group III, and Group V; ‖Significant differences were found between this group and Group V; ¶Significant differences were found between this group and Group IV and Group V. MANOVA: Multivariate analysis of variance; SD: Standard deviation.

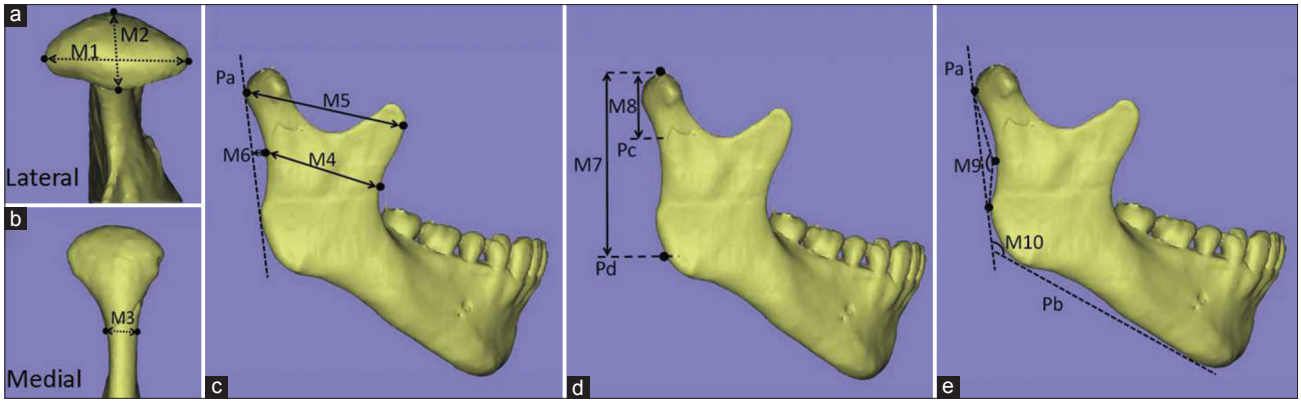


**Figure 3:** Definitions of measurements of mandibular ramus flexure. (a) M1: Condylar head width. M2: Condylar anteroposterior diameter (top view, right side). (b) M3: Condylar neck width (back view, right side). (c) M4: Minimum ramus breadth. M5: Maximum ramus breadth. M6: Mandibular flexure depth (lateral view, right side). (d) M7: Ramus height. M8: Condylar height. (e) M9: Condylar angle. M10: Mandibular angle.

**Table 5: Influence of each parameter on diacapsular fracture (Group I, Group II, and Group III)**

| Parameters | Group I vs. Group II | | | Group I vs. Group III | | | Group II vs. Group III | | |
|---|---|---|---|---|---|---|---|---|---|
| | *ORs* | 95% *CI* | *P* | *ORs* | 95% *CI* | *P* | *ORs* | 95% *CI* | *P* |
| M1 | 1.627 | 1.123–2.359 | 0.012* | 1.705 | 1.170–2.484 | 0.017* | 0.747 | 0.542–1.029 | 0.460 |
| M3 | 0.913 | 0.461–1.809 | 0.543 | 1.107 | 0.575–2.130 | 0.761 | 0.909 | 0.439–1.881 | 0.797 |
| M1/M2 | 1.034 | 0.876–1.220 | 0.013* | 1.185 | 0.973–1.443 | 0.097 | 1.202 | 0.959–1.506 | 0.301 |
| M1/M3 | 1.149 | 0.938–1.407 | 0.619 | 1.128 | 0.927–1.373 | 0.321 | 1.199 | 0.324–4.441 | 0.786 |
| M8/M7 | 0.934 | 0.820–1.064 | 0.303 | 1.006 | 0.863–1.173 | 0.682 | 1.077 | 0.927–1.252 | 0.195 |
| M10 | 0.956 | 0.877–1.042 | 0.305 | 0.869 | 0.780–0.968 | 0.011* | 0.909 | 0.821–1.007 | 0.044* |

**P*<0.05. 95% *CI*s, and *P* values are given for all variables. *OR*s: The association between parameters and diacapsular fracture. *ORs*: Odds ratios; *CI*s: Confidence intervals.

**Table 6: Influence of each parameter on condylar neck fracture, condylar base fracture, and diacapsular fracture (Group I, Group II, and Group III)**

| Parameters | Group IV vs. Group I + II + III | | | Group V vs. Group I + II + III | | | Group IV vs. Group V | | |
|---|---|---|---|---|---|---|---|---|---|
| | *ORs* | 95% *CI* | *P* | *ORs* | 95% *CI* | *P* | *ORs* | 95% *CI* | *P* |
| M1 | 1.027 | 0.798–1.322 | 0.837 | 0.803 | 0.632–1.020 | 0.072 | 1.339 | 0.972–1.843 | 0.074 |
| M3 | 0.382 | 0.203–0.720 | 0.003* | 0.851 | 0.531–1.365 | 0.503 | 0.436 | 0.218–0.874 | 0.019* |
| M1/M2 | 0.872 | 0.745–1.020 | 0.087 | 0.874 | 0.759–1.006 | 0.061 | 1.009 | 0.839–1.214 | 0.921 |
| M1/M3 | 1.229 | 1.063–1.420 | 0.005* | 1.014 | 0.885–1.162 | 0.841 | 1.223 | 1.034–1.447 | 0.014* |
| M8/M7 | 1.006 | 0.881–1.149 | 0.927 | 0.855 | 0.763–0.959 | 0.007* | 1.041 | 0.811–1.094 | 0.433 |
| M10 | 1.023 | 0.929–1.126 | 0.647 | 1.095 | 1.008–1.189 | 0.031* | 0.919 | 0.830–1.018 | 0.222 |

**P*<0.05. *P* values are given for all variables. *ORs*: The association between parameters and diacapsular fracture. *CI*: Confidence interval; *ORs*: Odds ratios.

associated with M1 (*OR* = 1.627, 95% *CI*: 1.123, 2.359) and M1/M2 (*OR* = 1.034, 95% *CI*: 0.876, 1.220). When compared to Type C condylar head fractures, Type A fractures were positively associated with M1 (*OR* = 1.705, 95% *CI*: 1.170, 2.484) and negatively associated with M10 (*OR* = 0.869, 95% *CI*: 0.780, 0.968). Type B condylar head fractures were negatively associated with M10 (*OR* = 0.909, 95% *CI*: 0.821, 1.007) as compared to Type C fractures.

Similarly, the results shown in Table 6 revealed that condylar neck fractures (compared to condylar head fractures) were negatively associated with M3 (*OR* = 0.382, *CI*: 0.203, 0.720) and positively associated with M1/M3 (*OR* = 1.229, 95% *CI*: 1.063, 1.420). Condylar base fractures (compared to condylar head fractures) were positively associated with M10 (*OR* = 1.095, 95% *CI*: 1.008, 1.189) and negatively associated with M8/M7 (*OR* = 0.855, 95% *CI*: 0.763, 0.959). In addition, condylar neck fractures were negatively associated with M3 (*OR* = 0.436, 95% *CI*: 0.218, 0.874) and positively associated with M1/M3 (*OR* = 1.223, 95% *CI*: 1.034, 1.447) as compared to condylar base fractures.

## Discussion

The present study was an attempt to verify clinical observations. Theoretically, condylar fractures caused by a parasymphyseal impact should be the same on both sides. However, in clinical practice, the patterns vary between the left and right sides because the factors that result in the fractures are complex and include the direction, intensity, and location of the external force and the biomechanical properties of the mandible.[22] To standardize the results of trauma, only patients who had the same condylar fracture on each side as a result of a parasymphyseal impact were included in the study.[23]

The development of CASS has been rapid and has provided valuable new insights for the evaluation of soft and hard tissues during craniomaxillofacial surgery.[24] In this study, mandibular anatomical morphology was precisely reconstructed to that before injury using the CASS technique. The morphological characteristics were quantified by measuring 3D reconstruction models. The accuracy and validity of 3D reconstruction models has been reported by several authors.[25,26]

Our results showed that Type A condylar head fractures are positively associated with the condylar head width and the ratio of condylar head width to condylar anteroposterior diameter. This means that people who have a high ratio of condylar head width to condylar anteroposterior diameter, or a greater than normal condylar head width, are more likely to have a Type A condylar head fracture after parasymphyseal impact. It is reasonable to suggest that a relatively applanate, or an outgrown condylar head, could lead to a Type A condylar head fracture after a parasymphyseal impact.

The results also showed that condylar neck fractures are closely related to the width of condylar neck and the ratio of condylar head width to condylar neck width. According to the multinomial logistic regression analysis, a narrow condylar neck, or a relatively broad condylar head, contributes to

the greater fragility of condylar neck, and biomechanical mechanisms could explain this phenomenon. The condylar neck is a weak point of mandible, and some studies using a simulated standard frontal impact acting on symphysis region have indicated that there is a concentration of stress on the condylar neck.[9,27] Hence, in our opinion, the more narrow condylar neck and broad condylar head, the more easily a fracture can occur.

Furthermore, the mandibular angle degree was positively associated with condylar base fractures and negatively associated with Type A and Type B condylar head fractures. This means that individuals with a larger mandibular angle are more prone to experience condylar base fractures. On the other hand, individuals with a smaller mandibular angle are more likely to develop Type A or Type B condylar head fractures. In addition, the results of our study also demonstrated that a greater condylar height to ramus height ratio decreases the likelihood of a condylar base fracture but increases the probability of a condylar head fracture. The different patterns of condylar fractures are caused by individual differences in stress concentration regions, and biomechanics, and these are closely associated with the anatomical features of the condyles.

The condylar fractures after parasymphyseal impact are indirect fractures caused by different mechanical stress distribution in the mandibular body and ramus, which are correlated with mandibular and chin morphological characteristics . It is well known that changes in the ramus morphology may affect the force transmission. In this study, parameters such as mandibular angle and the ratio of condylar height to ramus height are closely related to fracture pattern,which suggested that the above parameters may be some key factors which could decide the mechanical stress distribution in mandible and lead to different condylar fracture pattern finally, we will investigate this phenomena in subsequent works with FEA method.

MANOVA, and its *post hoc* analysis (LSD test), was used to identify variables significantly related to fracture patterns. As there were five categorical outcomes, we used multinomial logistic regression analysis to describe the possible relationships between the selected six relevant parameters and five fracture patterns.[28,29] In this study, multinomial logistic regression model is valid and fits the data well.

There are some limitations to this study. First, the sample size was relatively small. Second, we did not perform a FEA to support and explain the results. Other factors, such as other anatomical characteristics, surface area at the point of impact, action of the masticatory muscles, teeth occlusion, and condylar position during the injury, might influence the condylar fracture pattern.

It is important to study this subject to ensure appropriate treatment is provided for patients with condylar fractures, and this clinical investigation provides more information than FEA alone. The parameters identified must be considered in the decision-making process for fracture treatment and orthognathic surgery, such as whether to perform a mandibular angle sagittal split osteotomy, or sagittal split ramus osteotomy, and mandibular angle osteotomy. Several studies have shown that orthognathic surgery itself can occasionally lead to condylar fractures and carries some degree of risk. Beside the risk from the gross surgical procedure, the valuable parameters that can affect the condylar fracture patterns are other important factors.

In conclusion, the results of this study demonstrate that condylar fracture patterns are closely associated with the anatomical features of condyles, when the injury is due to a parasymphyseal impact. The internal factors that influence condylar fracture are many, and this study only focused on anatomical morphological characteristics. Future studies should include additional factors such as stress distribution, bone density, and masticatory muscle effects.


## Financial support and sponsorship

This work was supported by research grants from the National Natural Science Foundation of China (No.31570950,31070833, and 10502037).


## Conflicts of interest

There are no conflicts of interest.

## References


1. Lieger O, Zix J, Kruse A, Iizuka T. Dental injuries in association with facial fractures. J Oral Maxillofac Surg 2009;67:1680-4. doi: 10.1016/j.joms.2009.03.052.
2. Gassner R, Tuli T, Hächl O, Rudisch A, Ulmer H. Cranio-maxillofacial trauma: A 10 year review of 9,543 cases with 21,067 injuries. J Craniomaxillofac Surg 2003;31:51-61. doi: 10.1016/S1010-5182(02)00168-3.
3. Erol B, Tanrikulu R, Görgün B. Maxillofacial fractures. Analysis of demographic distribution and treatment in 2901 patients (25-year experience). J Craniomaxillofac Surg 2004;32:308-13. doi: 10.1016/j.jcms.2004.04.006.
4. Zachariades N, Mezitis M, Mourouzis C, Papadakis D, Spanou A. Fractures of the mandibular condyle: A review of 466 cases. Literature review, reflections on treatment and proposals. J Craniomaxillofac Surg 2006;34:421-32. doi: 10.1016/j.jcms.2006.07.854.
5. Zhou H, Lv K, Yang R, Li Z, Li Z, *et al.* Mechanics in the production of mandibular fractures: A clinical, retrospective case-control study. PLoS One 2016;11:e0149553. doi: 10.1371/journal.pone.0149553.
6. Park KP, Lim SU, Kim JH, Chun WB, Shin DW, Kim JY, *et al.* Fracture patterns in the maxillofacial region: A four-year retrospective study. J Korean Assoc Oral Maxillofac Surg 2015;41:306-16. doi: 10.5125/jkaoms.2015.41.6.306.
7. Ellis E 3rd, Moos KF, el-Attar A. Ten years of mandibular fractures: An analysis of 2,137 cases. Oral Surg Oral Med Oral Pathol 1985;59:120-9. doi: 10.1016/0030-4220(85)90002-7.
8. Lei T, Xie L, Tu W, Chen Y, Tang Z, Tan Y. Blast injuries to the human mandible: Development of a finite element model and a preliminary finite element analysis. Injury 2012;43:1850-5. doi: 10.1016/j.injury.2012.07.187.
9. Gallas Torreira M, Fernandez JR. A three-dimensional computer model of the human mandible in two simulated standard trauma situations. J Craniomaxillofac Surg 2004;32:303-7. doi: 10.1016/j.jcms.2004.04.008.
10. Murakami K, Yamamoto K, Sugiura T, Kawakami M, Kang YB, Tsutsumi S, *et al.* Effect of clenching on biomechanical response of human mandible and temporomandibular joint to traumatic force analyzed by finite element method. Med Oral Patol Oral Cir Bucal 2013;18:473-8. doi: 10.4317/medoral.18488.
11. Lü YL, Lou HD, Rong QG, Dong J, Xu J. Stress area of the

mandibular alveolar mucosa under complete denture with linear occlusion at lateral excursion. Chin Med J (Engl) 2010;123:917-21. doi: 10.3760/cma.j.issn.0366-6999.2010.07.028.
12. Huelke DF, Harger JH. Maxillofacial injuries: Their nature and mechanisms of production. J Oral Surg 1969;27:451-60.
13. Antic S, Vukicevic AM, Milasinovic M, Saveljic I, Jovicic G, Filipovic N, *et al.* Impact of the lower third molar presence and position on the fragility of mandibular angle and condyle: A Three-dimensional finite element study. J Craniomaxillofac Surg 2015;43:33-40. doi: 10.1016/j.jcms.2015.03.025.
14. Xin P, Jiang B, Dai J, Hu G, Wang X, Xu B, *et al.* Finite element analysis of type B condylar head fractures and osteosynthesis using two positional screws. J Craniomaxillofac Surg 2014;42:482-8. doi: 10.1016/j.jcms.2013.06.006.
15. Bayome M, Park JH, Kook YA. New three-dimensional cephalometric analyses among adults with a skeletal class I pattern and normal occlusion. Korean J Orthod 2013;43:62-73. doi: 10.4041/kjod.2013.43.2.62.
16. Tucker S, Cevidanes LH, Styner M, Kim H, Reyes M, Proffit W, *et al.* Comparison of actual surgical outcomes and 3-dimensional surgical simulations. J Oral Maxillofac Surg 2010;68:2412-21. doi: 10.1016/j.joms.2009.09.058.
17. Lindahl L. Condylar fractures of the mandible. I. Classification and relation to age, occlusion, and concomitant injuries of teeth and teeth-supporting structures, and fractures of the mandibular body. Int J Oral Surg 1977;6:12-21. doi: 10.1016/S0300-9785(77)80067-7.
18. Neff A, Mühlberger G, Karoglan M, Kolk A, Mittelmeier W, Scheruhn D, *et al.* Stability of osteosyntheses for condylar head fractures in the clinic and biomechanical simulation. Mund Kiefer Gesichtschir 2004;8:63-74. doi: 10.1007/s10006-004-0529-9.
19. Lee M, Kanavakis G, Miner RM. Newly defined landmarks for a three-dimensionally based cephalometric analysis: A retrospective cone-beam computed tomography scan review. Angle Orthod 2015;85:244. doi: 10.2319/021814-120.1.
20. Kim EJ, Ki EJ, Cheon HM, Choi EJ, Kwon KH. 3-dimensional analysis for class III malocclusion patients with facial asymmetry. J Korean Assoc Oral Maxillofac Surg 2013;39:168-74. doi: 10.5125/jkaoms.2013.39.4.168.
21. de Oliveira AE, Cevidanes LH, Phillips C, Motta A, Burke B, Tyndall D. Observer reliability of three-dimensional cephalometric landmark identification on cone-beam computerized tomography. Oral Surg Oral Med Oral Pathol Oral Radiol Endod 2009;107:256-65. doi: 10.1016/j.tripleo.2008.05.039.
22. Franklyn M, Field B. Experimental and finite element analysis of tibial stress fractures using a rabbit model. World J Orthop 2013;4:267-78. doi: 10.5312/wjo.v4.i4.267.
23. Chacon GE, Larsen PE. Maxillofacial trauma: Principles of management of mandibular fractures. Petersons Principles of Oral and Maxillofacial Surgery. Hamilton, London UK; 2004. p. 401-33.
24. Hsu SS, Gateno J, Bell RB, Hirsch DL, Markiewicz MR, Teichgraeber JF, *et al.* Accuracy of a computer-aided surgical simulation protocol for orthognathic surgery: A prospective multicenter study. J Oral Maxillofac Surg 2013;71:128-42. doi: 10.1016/j.joms.2012.03.027.
25. Whyms BJ, Vorperian HK, Gentry LR, Schimek EM, Bersu ET, Chung MK. The effect of computed tomographic scanner parameters and 3-dimensional volume rendering techniques on the accuracy of linear, angular, and volumetric measurements of the mandible. Oral Surg Oral Med Oral Pathol Oral Radiol 2013;115:682-91. doi: 10.1016/j.oooo.2013.02.008.
26. Periago DR, Scarfe WC, Moshiri M, Scheetz JP, Silveira AM, Farman AG. Linear accuracy and reliability of cone beam CT derived 3-dimensional images constructed using an orthodontic volumetric rendering program. Angle Orthod 2008;78:387-95. doi: 10.2319/122106-52.1.
27. Bezerra TP, Silva Junior FI, Scarparo HC, Costa FW, Studart-Soares EC. Do erupted third molars weaken the mandibular angle after trauma to the chin region? A 3D finite element study. Int J Oral Maxillofac Surg 2013;42:474-80. doi: 10.1016/j.ijom.2012.10.009.
28. Greene WH. Econometric Analysis. 7th ed. Boston: Pearson Education; 2012. p. 803-6.
29. Chan YH. Biostatistics 202: Logistic regression analysis. Singapore Med J 2004;45:149-53.